arXiv:0905.0151v1 [quant-ph] 1 May 2009

Creating and observing N-partite entanglement with atoms

Mark S. Everitt, Martin L. Jones, Benjamin T. H. Varcoe, and Jacob A. Dunningham
School of Physics and Astronomy, University of Leeds, Leeds LS2 9JT, United Kingdom

(Dated: May 1, 2009.)

The Mermin inequality provides a criterion for experimentally ruling out local-realistic descriptions of multiparticle systems. A violation of this inequality means that the particles must be entangled, but does not, in general, indicate whether N-partite entanglement is present. For this, a stricter bound is required. Here we discuss this bound and use it to propose a scheme for demonstrating N-partite entanglement with Rydberg atoms in microwave cavities.

PACS numbers: 03.65.Ud 03.67.Bg

Entanglement is a central feature of quantum mechanics and the key resource in a wide range of quantum information processing tasks. Being able to detect and characterize the entanglement present in a system is therefore an important challenge for physicists. The first mathematically sharp method of detecting entanglement for pairs of particles was proposed by John Bell in 1964 [1]. His now-famous inequality provided an unambiguous way of distinguishing quantum-mechanical predictions from those of local realistic models. Multiparticle generalizations of the Bell inequality were subsequently provided by Mermin [2] and others [3, 4, 5]. These can be used to rule out local-realistic models for N-particle systems and are also interesting because there is a close relationship between their violation and the security of N-partner quantum communications [6].

In general, a violation of these inequalities means that the particles must be entangled. In fact, by placing a stricter bound on the inequality [7, 8, 9] it is even possible to determine what class of entanglement is present from 2-entangled to N-entangled states. This method has been used to experimentally confirm three-body entanglement for photons [10]. In this Letter we discuss the conditions required to demonstrate N-partite entanglement and show how it could be generated and detected in atomic systems. We begin by reviewing the Mermin inequality and discussing how N-partite entangled states could be generated with Rydberg atoms in microwave cavities. We then demonstrate how all the terms in the Mermin inequality could be measured and consider some of the practical issues surrounding such an implementation.

It is helpful to start with a brief overview of the Mermin inequality [2]. For this, we consider an N-particle GHZ state of the form [23],

$$|\Phi\rangle_N = \frac{1}{\sqrt{2}}\big(|\underbrace{gg\cdots g}_{N}\rangle + |\underbrace{ee\cdots e}_{N}\rangle\big), \tag{1}$$

where g or e in the jth position denotes that the jth particle is in the ground or excited state. In an experiment, these N particles would be spatially separated and measurements made on each of them. We note that the GHZ state, $|\Phi\rangle_N$, is an eigenstate of the operator,

$$A_N = \frac{1}{2}\left(\prod_{j=1}^{N}(\sigma_x^j + i\sigma_y^j) + \prod_{j=1}^{N}(\sigma_x^j - i\sigma_y^j)\right) \tag{2}$$

with eigenvalue 2^{N-1}, where σ_x^i and σ_y^i are respectively the x and y Pauli spin matrices acting on the jth particle. Expanding, $F = \langle\Psi|A_N|\Psi\rangle$, for some general N-particle state $|\Psi\rangle$, one finds,

$$\begin{aligned} F = 1 \;&-\; \langle\Psi|\sigma_y^1\sigma_y^2\sigma_x^3\sigma_x^4\cdots\sigma_x^N|\Psi\rangle - \cdots \\ &+\; \langle\Psi|\sigma_y^1\cdots\sigma_y^4\sigma_x^5\cdots\sigma_x^N|\Psi\rangle + \cdots \\ &-\; \langle\Psi|\sigma_y^1\cdots\sigma_y^6\sigma_x^7\cdots\sigma_x^N|\Psi\rangle - \cdots \\ &+\; \cdots, \end{aligned} \tag{3}$$

where each line of (3) contains all distinct permutations of the operators in the term shown on that line. Only terms with an even number of σ_y operators are non-zero. For the GHZ state, we have $F = {}_N\langle\Phi|A_N|\Phi\rangle_N = 2^{N-1}$.

We would now like to find the corresponding value of F for a local hidden-variable state. Following Mermin, we consider the case where the measured distribution functions, $P_{\mu_1\cdots\mu_N}(m_1\cdots m_N)$, where $\mu_j \in \{x, y\}$ and $m_j \in \{g, e\}$, that describes the 2^{N-1} measurements that must be performed to yield the correlations in (3), can be written in the conditionally independent form,

$$P_{\mu_1\cdots\mu_N}(m_1\cdots m_N) = \int d\lambda\rho(\lambda)\left[p^1_{\mu_1}(m_1,\lambda)\cdots p^N_{\mu_N}(m_N,\lambda)\right] \tag{4}$$

where $p^i_{\mu_i}(m_i,\lambda)$ is the probability distribution of results for a measurement in the μ_i basis on particle i. This general hidden-variable form attributes the correlations to some unspecified set of parameters, λ, common to all N particles, with distribution $\rho(\lambda)$. It accounts for correlations in terms of information jointly available to the particles when they left their common source. An analysis similar to that of Mermin's shows that such a local hidden-variable state has the bounds [2],

$$\begin{aligned} F &\le 2^{N/2}, && N \text{ even}, \\ F &\le 2^{(N-1)/2}, && N \text{ odd}. \end{aligned} \tag{5}$$

We see that the GHZ state, $|\Phi\rangle_N$, for which $F = 2^{N-1}$, violates (5) by an exponential amount.

A violation of inequality (5) demonstrates that the particles are entangled, but does not guarantee N-partite entanglement [11]. For this, a tighter bound is needed, which can be found as follows. We assume that there is, at most, $(N-1)$-partite entanglement in the system. This means that the state of one of the lattice sites (say the first one) factorizes and the expectation value of the corresponding operator factorizes in each term in (3). Then using the fact that all expectation values disappear if they contain an odd number of σ_y operators, it is straightforward to show that we are left with:

$$F = \langle\sigma_x\rangle F_{N-1} \leq 2^{N-2}, \tag{6}$$

where the last step follows because $\langle\sigma_x\rangle \leq 1$ and $F_{N-1} \leq 2^{N-2}$. This agrees with the condition found for three particles in [8]. Any state that violates (6) must have at least N-partite entanglement.

The aim of an experiment would be to measure all the expectation values in (3) and see firstly whether their sum violates the bound given by (5), in which case entanglement is present, and secondly whether it violates the bound given by (6) in which case N-partite entanglement is present. We now discuss how such a scheme could be implemented.

The first step is to create a GHZ of the form of (1). To do this we use a modified version of the scheme found in [12]. In short we start with N atoms of ^{85}Rb, each initially in the Rydberg state 63P. Using resonant microwave fields transitions can be driven to the levels 61D and 62P. We shall refer to 63P as $|e\rangle$, the relative excited state, and 61D as $|g\rangle$, the relative ground state. These form the basis used to construct the GHZ state. The state 62P is referred to as $|i\rangle$, an auxiliary state. The state $|e\rangle$ is produced using a three step laser excitation. Zheng and Guo demonstrate in their paper [13] that using three states like this, with a cavity detuned from the $|e\rangle \leftrightarrow |g\rangle$ transition it is possible to create an EPR state. This was later demonstrated experimentally by Osnaghi et al. [14]. Recently this scheme was extended in [12] to show that using the same states and $N-1$ cavities in a line it is possible to produce a GHZ state of N atoms [24]. An alternative has been demonstrated by Rauschenbeutel et al. [15].

The scheme in [12] starts with all atoms initially in the state $|e\rangle$. These atoms are produced on demand [16]. Next all atoms are rotated to the state $|+\rangle = (|g\rangle + |e\rangle)/\sqrt{2}$ using a microwave field resonant with the $|e\rangle \leftrightarrow |g\rangle$ transition. This corresponds to a rotation about the x-axis on the Bloch sphere. The Hamiltonian used to implement this is

$$H_I = \hbar\Omega\left(\hat{\sigma}^+ + \hat{\sigma}^-\right), \tag{7}$$

where Ω is the coupling strength of the atom with the field and $\hat{\sigma}^+$ and $\hat{\sigma}^-$ are the atomic raising and lowering operators. The amplitudes of the atom given as $a(t)|g\rangle + b(t)|e\rangle$ evolve according to the equations

$$\begin{aligned} a(t) &= a_0\cos(\Omega t) - ib_0\sin(\Omega t) \\ b(t) &= b_0\cos(\Omega t) - ia_0\sin(\Omega t), \end{aligned} \tag{8}$$

which is equivalent to a rotation about the x-axis.

The first atom, which will interact with each other atom in turn, then passes through another microwave field (labelled as b in Fig. 1) which is resonant with the transition $|e\rangle \leftrightarrow |i\rangle$ leaving the first atom in the state $(|g\rangle + |i\rangle)/\sqrt{2}$. The first atom now interacts with the second in a high-Q microwave cavity. This cavity is detuned from the $|e\rangle \leftrightarrow |g\rangle$ resonance. The four possible states that may interact are shown in the left column of table I. The first two states in the left column of the table are modelled using a two atom Tavis-Cummings model with large detuning. With a zero photon field [17] this can be solved to give the interaction

$$\begin{aligned} &|g,e\rangle \mapsto \mathrm{e}^{-i\gamma t}\left[\cos(\gamma t)|g,e\rangle - i\sin(\gamma t)|e,g\rangle\right] \\ &|g,g\rangle \mapsto |g,g\rangle \end{aligned} \tag{9}$$

where $\gamma = g^2/\Delta$, g is the atom-field coupling constant and Δ is the detuning. As the field is detuned from the transition, excited atoms can only virtually excite the field, effectively coupling the atoms together and allowing an excitation to be passed between atoms. The zero photon stipulation is satisfied in the laboratory by cryogenically cooling the cavity, and possibly by preceding the experiment with a chain of atoms in the state $|g\rangle$ to unload the field. The second two states in the left column of table I each have one atom in the state $|i\rangle$, for which all transitions are so far from the cavity resonance that we may assume that it does not contribute to the dynamics of the system. This leaves one atom and the detuned field, which is modelled using the Jaynes-Cummings model. In the case of zero photons and large detuning the evolution of these two states is given by

$$\begin{aligned} &|i,e\rangle \mapsto \mathrm{e}^{-i\gamma t}|i,e\rangle \\ &|i,g\rangle \mapsto |i,g\rangle, \end{aligned} \tag{10}$$

For creating a GHZ state we choose the interaction time and detuning such that $t = \pi/4\gamma$. For each interaction this provides the right hand side of the truth table I. After the interaction with the first atom each atom emerging from each cavity is rotated so that $|g\rangle \to |+\rangle$ and $|e\rangle \to |-\rangle = (|g\rangle - |e\rangle)/\sqrt{2}$. After the first atom emerges from the final cavity it enters a microwave field that drives the transition $|i\rangle \leftrightarrow |e\rangle$ so that the atom is left with no amplitude in $|i\rangle$. The atoms are now in a GHZ state ready for use. Figure 1 demonstrates the construction of a three atom GHZ state. It is also possible to generate larger entangled structures with more elaborate cavity arrays [18].

Input	Output
$\lvert g,g\rangle$	$\lvert g,g\rangle$
$\lvert g,e\rangle$	$\lvert g,e\rangle$
$\lvert i,g\rangle$	$\lvert i,g\rangle$
$\lvert i,e\rangle$	-$\lvert i,e\rangle$

TABLE I: The truth table for the collisional phase gate introduced in [13].

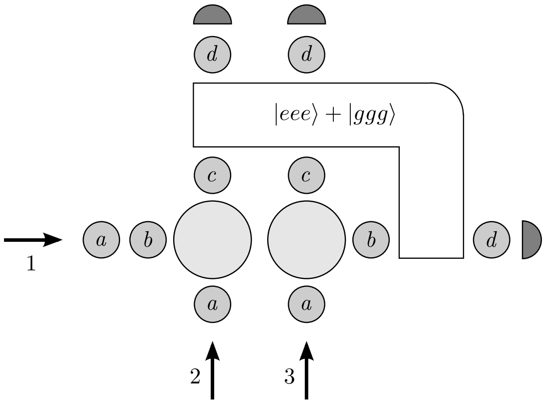

FIG. 1: This example produces a three party GHZ state of atoms. Atoms approach as indicated by arrows to coincide in each cavity (large circles). Initially all atoms are in state $\lvert e\rangle$. The rotation zones labelled a take $\lvert e\rangle$ to $\lvert +\rangle$ and c take $\lvert e\rangle$ to $\lvert -\rangle$ and $\lvert g\rangle$ to $\lvert +\rangle$. Those zones labelled b act on the first atom (traveling horizontally) to switch $\lvert e\rangle$ components of the state to $\lvert i\rangle$, the auxiliary state, and vice versa. The enclosed region is where the GHZ state exists. The zones labelled d are arbitrary rotations used to study the state before measurement.

Now we would like to make measurements on this system that correspond to the terms in (3). This involves making measurements on each qubit in the basis of the eigenstates of σ_x and σ_y, i.e. $\lvert g\rangle \pm \lvert e\rangle$ and $\lvert g\rangle \pm i\,\lvert e\rangle$ respectively. The rotations take place in the regions labelled d in Figure 1. The rotation in the basis of σ_x has already been discussed, and only one other rotation on the Bloch sphere is needed to realise a rotation in the basis of σ_y.

The second operation we use is a rotation about the z-axis of the Bloch sphere, R_z. This can be implemented simply by applying an electric field to the atom. This effectively increases the transition energy between the levels of the atom and results in a different phase evolution for the two states. This technique has been experimentally demonstrated with sodium Rydberg atoms by Ryabtsev et al. [19]. They applied a resonant microwave pulse to perform an x-rotation between two sodium Rydberg atoms followed by a Stark shift z-rotation and another x-rotation. This combination of interactions allowed them to perform Ramsey interferometry of the R_z operation applied by the Stark shift. Their results confirmed that they has successfully implemented the phase operation R_z and that it is coherent [19].

For Rydberg states of alkali metals the Stark shift varies approximately quadratically with the electric field strength [20],

$$\delta_{g,e} \propto -\alpha_{g,e} E^2 \,, \tag{11}$$

where $\alpha_{g,e}$ is the polarizability of the ground or excited state of the atom and E is the amplitude of the electric field. The polarizability of the two states will be different, so the relative phase shift will be given by

$$\Theta = \epsilon(\alpha_g - \alpha_e) E^2 \,, \tag{12}$$

where ϵ is a factor calculated by integrating over the pulse shape of the electric field. Applying the electric field for some time t, the state of the atom evolves as

$$a\,\lvert e\rangle + b\,\lvert g\rangle \mapsto \mathrm{e}^{-i\Theta t} a\,\lvert e\rangle + b\,\lvert g\rangle \,. \tag{13}$$

This corresponds to a rotation about the z-axis, where Θt is the angle of rotation.

Now, in order to measure an atom in the σ_x basis, we simply apply the resonant microwave field to implement a rotation of the state by $\pi/2$ about the y-axis and then measure the atom to see whether it is in the state $\lvert g\rangle$ or $\lvert e\rangle$. We can see that this works because the rotation maps the eigenstates of σ_x directly onto the states $\lvert g\rangle$ and $\lvert e\rangle$. Similarly, to measure in the σ_y basis we apply a $\pi/2$ rotation about the z-axis (using the Stark shift), then a $\pi/2$ rotation about the y-axis, and then measure the atom to see whether it is in $\lvert g\rangle$ or $\lvert e\rangle$. Measuring Rydberg atoms is discussed by Gallagher [21]. The particular measurement process that is useful in this experiment, state selective field ionisation, is described in [17].

So far, we have considered the case of detecting N-partite entanglement by making measurements on the total system. However, it should also be possible to detect multiparticle entanglements on subsystems. Suppose we consider only the atoms that pass through the first $\tilde{N}$ cavities in Figure 1. We ensure that all the σ_y measurements are made on these $\tilde{N}$ atoms and that only σ_x measurements are made on the remaining atoms. In this case, the expectation value for a general term in (3) has the form,

$$\begin{aligned} &{}_N\langle\Phi\rvert\, \overbrace{\sigma_y^1 \cdots \sigma_y^j \sigma_x^{j+1} \cdots \sigma_x^{\tilde{N}}}^{\text{First } \tilde{N} \text{ sites}}\, \sigma_x^{\tilde{N}+1} \cdots \sigma_x^N \lvert\Phi\rangle_N \\ &\quad = {}_{\tilde{N}}\langle\Phi\rvert \sigma_y^1 \cdots \sigma_y^j \sigma_x^{j+1} \cdots \sigma_x^{\tilde{N}} \lvert\Phi\rangle_{\tilde{N}} = i^j, \end{aligned} \tag{14}$$

where any permutation of the first $\tilde{N}$ operators in either expression does not change the result and j is even. From (14), we see that restricting all the σ_y measurements to the first $\tilde{N}$ atoms gives the same results as the full Mermin inequality for a state of the form of (1), but with $\tilde{N}$ (rather than N) atoms. From this observation, it follows that we have $F = 2^{\tilde{N}-1}$, and the bound for $(\tilde{N}-1)$-partite entanglement is

$$F \leq 2^{\tilde{N}-2}. \tag{15}$$

The corresponding bound for the hidden variable model follows easily from (4) since the joint probability for N sites can be reduced to a joint probability for $\tilde{N}$ sites simply by integrating over $m_{\tilde{N}+1}, \cdots, m_N$. This gives,

$$\begin{aligned} & P_{\mu_1 \cdots \mu_{\tilde{N}}}(m_1 \cdots m_{\tilde{N}}) \\ & \quad = \int d\lambda \rho(\lambda) \left[p^1_{\mu_1}(m_1, \lambda) \cdots p^{\tilde{N}}_{\mu_{\tilde{N}}}(m_{\tilde{N}}, \lambda) \right], \end{aligned} \tag{16}$$

i.e. the first $\tilde{N}$ sites do not depend on the measurement outcomes of the last $N - \tilde{N}$ sites. The rest of the argument follows that of Mermin [2] but with N replaced with $\tilde{N}$. This gives the hidden variable bounds as,

$$\begin{aligned} F &\leq 2^{\tilde{N}/2}, & \tilde{N} \text{ even}, \\ F &\leq 2^{(\tilde{N}-1)/2}, & \tilde{N} \text{ odd}. \end{aligned} \tag{17}$$

Comparing (17) and (15) with the result for a GHZ state, $F = 2^{\tilde{N}-1}$, we see that it is possible to rule out local-realistic models and detect $\tilde{N}$-partite entanglements on a part of the total state.

Finally we ought to comment on how noise affects these results since it is well-known that detector inefficiencies in particular give rise to the so-called detection loophole which can undermine our ability to exclude local-realistic descriptions using Bell-type inequalities. Braunstein and Mann [22] have considered this problem and shown that if the noise is sufficiently small, then the signal for violation grows exponentially faster with N than the noise. In particular, the noise per detector or per particle needs to be less than about 14%. This bodes well for the feasibility of the detection process.

Besides its significance in tests of quantum mechanics versus local realism, the scheme we have proposed could be an important tool in unambiguously creating and identifying genuine N-body entanglement in atomic systems.

This work was supported by the United Kingdom EPSRC through an Advanced Research Fellowship GR/S99297/01, Advanced Fellowship GR/T02331/01, Scholarship GR/T02324/01, Grant GR/S21892/01, a RCUK Fellowship, and the EuroQUASAR programme EP/G028427/1.

---

[1] J. S. Bell, Physics **1**, 195 (1964).

[2] N. D. Mermin, Physical Review Letters **65**, 1838 (1990).

[3] A. V. Belinskii and D. N. Klyshko, PhysicsUspekhi **163** (1993).

[4] N. Gisin, Physics Letters A **246**, 1 (1998), ISSN 03759601.

[5] R. F. Werner and M. M. Wolf, Physical Review A **64**, 032112 (2001).

[6] V. Scarani and N. Gisin, Physical Review Letters **87**, 117901 (2001).

[7] M. Seevinck and J. Uffink, Physical Review A **65**, 012107 (2001).

[8] G. Tóth, O. Gühne, M. Seevinck, and J. Uffink, Physical Review A **72**, 014101 (2005).

[9] S. Yu, Z. B. Chen, J. W. Pan, and Y. D. Zhang, Physical Review Letters **90**, 080401 (2003).

[10] Y. A. Chen, T. Yang, A. N. Zhang, Z. Zhao, A. Cabello, and J. W. Pan, Physical Review Letters **97**, 170408 (2006).

[11] A. Shimizu and T. Morimae, Physical Review Letters **95**, 090401 (2005).

[12] M. S. Everitt, M. L. Jones, and B. T. H. Varcoe, *Dephasing of entangled atoms as an improved test of quantum gravity* (2008), arXiv:0812.3052.

[13] S.-B. Zheng and G.-C. Guo, Physical Review Letters **85**, 2392 (2000).

[14] S. Osnaghi, P. Bertet, A. Auffeves, P. Maioli, M. Brune, J. M. Raimond, and S. Haroche, Physical Review Letters **87**, 037902 (2001).

[15] A. Rauschenbeutel, G. Nogues, S. Osnaghi, P. Bertet, M. Brune, J.-M. Raimond, and S. Haroche, Science **288**, 2024 (2000).

[16] S. Brattke, B. T. H. Varcoe, and H. Walther, Physical Review Letters **86**, 3534 (2001).

[17] B. G. Englert, M. Löffler, O. Benson, B. Varcoe, M. Weidinger, and H. Walther, Fortschritte der Physik **46**, 897 (1998).

[18] P. J. Blythe and B. T. H. Varcoe, New J. Phys. **8**, 231 (2006).

[19] I. I. Ryabtsev, D. B. Tretyakov, and I. I. Beterov, Journal of Physics B: Atomic, Molecular and Optical Physics **36**, 297 (2003).

[20] V. A. Davydkin, V. D. Ovsyannikov, and B. A. Zon, Laser Physics **3**, 449 (1993).

[21] T. F. Gallagher, *Rydberg Atoms (Cambridge Monographs on Atomic, Molecular and Chemical Physics)* (Cambridge University Press, 1994).

[22] S. L. Braunstein and A. Mann, Physical Review A **47**, R2427 (1993).

[23] This state and the subsequent analysis differs slightly from that put forward by Mermin. We choose to do the analysis for this particular state because it is the one most conveniently created by our proposed experimental scheme for Rydberg atoms.

[24] Alternatively we could use atoms at different velocities and a single cavity so that one atom is present during the passage of the other atoms, which are only present one at a time, effectively emulating multiple cavities.